Marine Pollution Bulletin 218 (2025) 118183

Contents lists available at ScienceDirect

Marine Pollution Bulletin

journal homepage: www.elsevier.com/locate/marpolbul

Photochemical treatment strategies for okadaic acid degradation: Effects of salinity, oxidants, and UV sources

Javier Moreno-Andrés [a,*], Sandra Lage [b], Ana Catarina Braga [c], Pedro Reis Costa [b,d]

[a] Department of Environmental Technologies, Faculty of Marine and Environmental Sciences, INMAR-Marine Research Institute, University of Cádiz, Campus Universitario Puerto Real, 11510 Puerto Real, Cádiz, Spain
[b] Centre of Marine Sciences (CCMAR/CIMAR LA), University of Algarve, Campus of Gambelas, 8005-139 Faro, Portugal
[c] S2AQUA— Collaborative Laboratory, Association for a Sustainable and Smart Aquaculture, Av. Ria Formosa Natural Park s/n, 8700-194 Olhão, Portugal
[d] IPMA - Portuguese Institute of the Sea and Atmosphere, Av. Brasília, 1449-006 Lisbon, Portugal

ARTICLE INFO

Keywords:
Phycotoxin
Seawater toxicity
Seawater treatment
UV-LED
Advanced oxidation processes

ABSTRACT

This study evaluates the degradation and detoxification of okadaic acid (OA), a marine biotoxin, through UV-assisted photochemical processes using environmentally relevant OA concentrations. Experiments were conducted in distilled water (DW) and artificial seawater (ASW), applying two UV sources: UV-LED (λ_{max} = 275 nm) and low-pressure mercury lamp (LP-Hg; λ = 254 nm), combined with hydrogen peroxide (HP), sodium peroxydisulfate (PDS), and potassium peroxymonosulfate (PMS). Photolysis alone was ineffective, and kinetic rate constants (k_{obs}; min^{-1}) followed the trend UV/PMS > UV/PDS > UV/HP for both UV sources. While all treatments showed high OA removal (>79 %) in DW, degradation was significantly reduced for HP (72.8 %–89.9 %) and PDS (67.8 %–76.6 %) in ASW. In contrast, UV/PMS efficacy improved in saline media, achieving rapid and effective degradation of OA, and reaching 99 % detoxification (PP2A activity) within 15 min. The main transformation product, norokadanone (*m/z* 757.453), formed via decarboxylation, showed significantly reduced toxicity compared to OA. These results confirm the suitability of sulfate radical-based processes (particularly UV/PMS) for OA mitigation in marine environments. In addition, this work highlights the critical role of water matrix composition in marine toxin treatment and supports the development of scalable, mercury-free strategies for effectively mitigating hazardous compounds in coastal environments.

1. Introduction

Marine phycotoxins, although produced by a limited number of microalgae species, pose significant risks to marine ecosystems, fisheries, and public health. The European Food Safety Authority (EFSA) classifies them into eight structural groups (Alexander et al., 2009; Visciano et al., 2016), with most being lipophilic, except for hydrophilic toxins like saxitoxins and domoic acid (Costa et al., 2014; González-Jartín et al., 2020). Over 300 lipophilic variants have been identified, some of which may occasionally bypass conventional desalination systems or accumulate in seafood, particularly bivalves (Li et al., 2021; Villacorte et al., 2021). Their ingestion may lead to various toxic effects, with diarrhetic shellfish poisoning (DSP), primarily caused by okadaic acid and dinophysistoxins, being a major concern for food safety (Braga et al., 2023; Fernández et al., 2019; Henigman et al., 2024; Rodríguez et al., 2015; Visciano et al., 2016).

The widespread presence of DSP toxins in coastal waters underscores the urgent need for effective monitoring and control (Bian et al., 2024; Costa et al., 2017). Okadaic acid (OA) is the primary DSP toxin posing food safety risks in shellfish farms in the Adriatic Sea (Henigman et al., 2024) and is the most common biotoxin on the Portuguese coast (Braga et al., 2023). Similar patterns are observed in Northern China (Sheng et al., 2025) or Spain (Fernández et al., 2019; Rodríguez et al., 2015). In the Mediterranean, about 75 % of toxic events are linked to DSP, primarily due to OA (Zingone et al., 2021).

OA contains a carboxyl group that confers slight water solubility, making it the predominant lipophilic phycotoxin in the water column (Li et al., 2024). Dissolved OA has been reported in surface seawater at concentrations ranging from 0.14 to 1780 ng/L in various regions (Bosch-Orea et al., 2017; Li et al., 2024; Sheng et al., 2025; Zhou et al., 2024). Besides, OA remains stable in seawater and interstitial water for extended periods (Blanco et al., 2018). Recent findings also suggest that

* Corresponding author.
E-mail address: javier.moreno@uca.es (J. Moreno-Andrés).

https://doi.org/10.1016/j.marpolbul.2025.118183
Received 9 April 2025; Received in revised form 7 May 2025; Accepted 17 May 2025
Available online 30 May 2025

dissolved OA may sorb onto floating plastic debris, potentially increasing its environmental mobility and bioavailability (Costa et al., 2020).

Coastal water intended for human consumption is typically desalinated, and while reverse osmosis can remove OA with 97–99.7 % efficiency (often requiring additional oxidation steps) evidence from full-scale operations during toxic bloom events remains limited (Kim et al., 2024; Villacorte et al., 2021). In aquaculture, natural depuration of OA in bivalves is slow and temperature-dependent, with marine heatwaves potentially disrupting toxin elimination (Dias et al., 2025). Alternative methods such as ozonation, thermal processing, or freezing remain challenging (Martinez-Albores et al., 2020; Reboreda et al., 2010). Therefore, additional treatment approaches are needed for confined or semi-closed systems, where OA can accumulate to hazardous levels, posing risks to food safety and industry productivity (Bian et al., 2024).

Few studies have focused on the degradation of marine lipophilic toxins like OA using physicochemical techniques. Adsorption efficiencies up to 40 % have been reported, though performance depends strongly on the toxin's functional groups (González-Jartín et al., 2020). Photolytic (Pan et al., 2020; Qiu et al., 2025) and photocatalytic-TiO_2 treatments (Camacho-Muñoz et al., 2020) have also been studied. OA photodegradation was slow under solar or UV-A radiation (Camacho-Muñoz et al., 2020; Pan et al., 2020), highlighting the need for more energetic UV-C sources. While photocatalysis showed >80 % removal in distilled water, efficiency declined in seawater, and residual toxicity of transformation products was still observed (Camacho-Muñoz et al., 2020). This aligns with other studies indicating that high salinity inhibits TiO_2-based treatments, raising concerns about their viability in marine environments (Levchuk et al., 2019; Porcar-Santos et al., 2020).

UV radiation is commonly applied in aquaculture and seafood depuration systems (Bian et al., 2024; FAO, 2008). Recent developments in UV-based water treatment highlight mercury-free LEDs as promising alternatives due to their design flexibility, long lifespan, and alignment with Minamata Convention goals. Although their efficiency at lower wavelengths is still limited, further improvements are expected (Martín-Sómer et al., 2023). However, UV radiation alone is often insufficient for effective pollutant degradation and typically requires combination with oxidants in photochemical Advanced Oxidation Processes (AOPs). While such processes have been widely studied for freshwater cyanotoxins (He et al., 2013; Lee et al., 2019; Sha et al., 2024), their application to marine phycotoxins remains scarcely explored. Evaluating the viability of these approaches under saline conditions and with novel UV sources is therefore essential to advance marine water treatment strategies.

This study evaluates the degradation and detoxification of OA in seawater using UV-assisted photochemical processes, examining the combined effects of salinity, oxidant type (H_2O_2, $S_2O_8^{2-}$, HSO_5^-), and UV source. Special attention is given to the use of emerging UV-LED technologies as alternatives to mercury-based lamps (LP-Hg). By assessing their performance under realistic saline conditions and analysing transformation products and residual toxicity, this work addresses a scarcely explored yet environmentally relevant scenario and contributes new insights into the applicability of AOPs for marine toxin mitigation.

2. Material and methods

2.1. Chemicals and reagents

Okadaic acid was obtained from Sigma Aldrich as Okadaic Acid, Potassium Salt (≥ 95 %). Methanol (LC-MS grade), acetonitrile (LC-MS grade), ammonium formate (99 % purity) from Fluka; Formic acid (98 %) from Roth. Water was purified using a Milli-Q 185 Plus system from Millipore. Artificial seawater was prepared with Instant Ocean® Sea Salt.

Reagents for photochemical processes were hydrogen peroxide (HP), H_2O_2, 30 %, ultrapure, Scharlau; sodium peroxydisulfate salt (PDS), $Na_2S_2O_8$, Panreac; and Peroxymonosulfate (PMS), obtained from Oxone© ($KHSO_5 \cdot 0.5KHSO_4 \cdot 0.5K_2SO_4$), Sigma-Aldrich;. Titanium (IV) oxysulfate solution (Sigma-Aldrich) and potassium iodide (KI, 99 %, Pharmpur, Scharlab) were used for determination of HP, PDS, and PMS.

OkaTest, ZeuLab, S.L., an enzymatic assay used to detect and quantify okadaic acid group toxins in shellfish, was used for determining the potential toxicity after the photochemical treatments.

2.2. UV reactor configuration

Irradiation experiments were performed with two similar collimated beam reactors distinguished according to the UV-C source: a low-pressure mercury lamp (LP-Hg, 10 W, λ_{max} = 254 nm; obtained from Wedeco Rex UV systems) and a UV-LED device (10.5 mW, peak emission at 265–285 nm, λ_{max} = 275 nm; obtained from Photolab LED275–0.01/300–0.03/365-1cb; APRIA Systems S.L., Spain). A detailed description of the reactor setup can be found in previous studies (Moreno-Andrés et al., 2018, 2023).

Each photoreactor contains a collimating tube equipped with a collimator lens (5.08 cm in diameter, focal length of 6 cm). Samples were placed in Petri dishes (internal diameter: 54 mm; volume capacity: 50 mL), and a magnetic stirrer was used to ensure continuous mixing during irradiation (Fig. S1).

To determine mean irradiance, measurements were taken using a radiometer (HD 2102.1, Delta OHM) equipped with a UV probe (Delta OHM LP471–UVBC). As the radiometer measures only the central beam intensity at the water surface, several correction factors were applied to estimate the average irradiance. These corrections were based on the standard protocol described by Bolton and Linden (2003). For the UV-LED source, it was considered a quasi-monochromatic emitter, as established by Pousty et al. (2022).

Considering the geometrical characteristics of the system (10 cm distance from lamp to water surface, Petri dish inner diameter: 54 mm, water depth: 30 mm), and the absorbance of the water matrix: 0.007 ± 0.002 at 254 nm (T_{254}: 98.40 % ± 0.31) and 0.006 ± 0.002 at 275 nm (T_{275}: 98.74 % ± 0.48); the reflection factor, Petri factor, water factor, and divergence factor were calculated (Bolton and Linden, 2003). These were then used to estimate the average irradiance within the solution for both UV sources, resulting in values of 0.378 ± 0.091and 0.072 ± 0.005 $mW \cdot cm^{-2}$ for LP-Hg and UV-LED respectively.

2.3. Photochemical degradation experiments

The experiments were conducted based on the type of UV radiation source (UV-LED and LP-Hg) and the chemical reagent used (HP, PDS, PMS) in two different water matrices: distilled water, DW (pH = 7.09; k = 370 μS/cm) and artificial seawater, ASW (pH = 8.22; k = 30.2 mS/cm), which was prepared by dissolving 30 g/L of Instant Ocean® Sea Salt in DW water. OA was spiked into the different aqueous matrices at $[OA]_0$ = 25 ng/mL, which is slightly higher than those reported in natural waters (0.14 to 1.78 ng/mL) (Bosch-Orea et al., 2017; Li et al., 2024; Zhou et al., 2024), but similar to those used in similar studies (10 ng/mL) that attained to potential concentrations estimated during a toxigenic red tide outbreak (Pan et al., 2020; Pepe-Vargas et al., 2024).

The experimental setup involved exposing aqueous samples (DW or ASW) in Petri dishes to the two UV radiation sources for specific exposure periods of up to 180 min under continuous stirring, which implies maximum UV-Doses of 4.08 J/cm^2 and 0.77 J/cm^2 for LP-Hg and UV-LED, respectively. When necessary, the chemical reagent (HP, PDS or PMS) was added in one time from stock solutions, in order to reach the concentration of 0.5 mM. This concentration was selected according to previous studies (He et al., 2013; Lee et al., 2019) and permits the comparison of the photo-chemical processes at equivalent molar concentrations assuring that the exhaustion of the reagent is avoided. Also, experiences in the absence of chemical reagents were performed, to address the possible photolysis of OA.

During the 180 min of UV radiation exposure, 1 mL aliquots were collected at selected time intervals to create a specific degradation curve for each combination of light source, chemical reagent, and water matrix. Additionally, experiments were conducted under similar conditions to observe the degradation of the chemical reagents (PDS, PMS, or HP), detect transformation products, and assess the associated toxicity.

2.4. Analytical methods

2.4.1. Sample preparation and LC-MS/MS analysis of okadaic acid

Extraction and clean-up of OA were carried out using solid-phase extraction (SPE), following the method described by Pan et al. (2020). Further details are provided in Supplementary Material, Text S1.

LC-MS/MS analysis was performed using an Agilent 1290 Infinity chromatograph coupled to an Agilent 6470 triple quadrupole mass spectrometer (Agilent Technologies, Germany). Detection was conducted according to the Standard Operating Procedure of the European Reference Laboratory for Marine Biotoxins for the determination of lipophilic marine biotoxins. Additional information is available in Supplementary Material, Text S2.

2.4.2. LC-HRMS analysis of okadaic acid and transformation products

Samples were also analyzed by Liquid Chromatography - High-Resolution Mass Spectrometry (LC-HRMS) with focus on transformation products but also to corroborate results of parent compound, OA (Costa et al., 2022).

OA and its transformation products identification were performed by generating accurate mass-extracted ion chromatograms (AM-XIC) with the calculated exact masses of the $[M + H]^+$ and $[M - H]^-$ ions in the correspondent full-scan LC- HRMS chromatograms and a mass extraction window of ±5 ppm (Text S3). In the absence of commercially available authentic standards for OA-transformation products, their unequivocal identification was performed according to their experimental exact mass (*m/z*) with a mass accuracy <5 ppm, accurate isotopic pattern, fragmentation spectra and retention time according to Table 1 (Camacho-Muñoz et al., 2020; Pan et al., 2020). The obtained concentrations of OA and its transformation products were estimated from the MS response to the OA certified reference material. Additional information is available in Supplementary Material, Text S3.

2.4.3. Protein phosphatase inhibition assay (PP2A activity test)

The toxicity of OA -group toxins was evaluated using the OkaTest assay (ZeuLab, S.L.), a method specifically developed for this toxin group. In this assay, samples were incubated with purified PP2A enzyme and a chromogenic substrate under standardized conditions. Enzymatic activity, inversely related to OA toxicity, was quantified by spectrophotometric measurement of the reaction product at 405 nm using a TECAN Infinite 200 Pro microplate reader.

2.4.4. Determination of oxidant concentrations (HP, PDS, PMS)

Analytical determination of HP, PDS and PMS was monitored through colorimetric methods with titanium (IV) oxysulfate solution (Method DIN 38402 H15) and potassium iodide (KI, 99 %, Pharmpur, Scharlab) for determination of PDS and PMS (Liang et al., 2008; Wacławek et al., 2015). Spectrophotometric measurements were performed with a UV-1600PC spectrophotometer (VWR).

Table 1
Okadaic acid transformation products $[M+ H] +$ and $[M - H]^-$ *m/z*.

Chemical formula	$[M+ H]^+$ *m/z*	$[M - H]^-$ *m/z*	References
$C_{18}H_{32}O_5$	329.322	327.218	Pan et al., 2020
$C_{25}H_{38}O_9$	483.259	481.244	Pan et al., 2020
$C_{27}H_{44}O_8$	497.311	495.296	Pan et al., 2020
$C_{36}H_{54}O_9$	631.384	629.370	Pan et al., 2020
$C_{43}H_{66}O_{11}$	759.468	757.453	Pan et al., 2020 & Camacho-Muñoz et al., 2020
$C_{44}H_{70}O_{14}$	819.455	821.469	Pan et al., 2020

2.5. Data treatment and statistical analysis

OA degradation followed in all cases a pseudo-first-order kinetic, which can be described as a function of time (Eq. (1)).

$$C = C_0 \cdot e^{-k \cdot t} \quad (1)$$

where C_0 is the initial concentration of OA, C is the concentration at a specific time t (min), k is the time-based kinetic constant (min^{-1}).

To check whether there were any differences in water matrix and chemical reagents, according to the UV-source applied for the degradation of OA, the time-based kinetic constant was analyzed by means of two-way ANOVA followed by Tukey's multiple comparisons test using GraphPad Prism version 8.0.0.

Using the data from OkaTest, the PP2A activity was measured and expressed as a percentage of total PP2 activity, with indication that PP2A activity increases as the concentration of OA decreases.

3. Results and discussion

3.1. Photolysis of okadaic acid

Single UV-radiation was tested for the abatement of OA in two different water matrices: distilled water (DW) and artificial seawater (ASW), using two UV sources: a low-pressure mercury lamp (LP-Hg) and a UV-LED system. Fig. 1 shows the percentage of photodegradation after 180 min of UV-C exposure, ccorresponding to maximum UV doses of 4.08 J/cm^2 and 0.77 J/cm^2 for LP-Hg and UV-LED, respectively. In all cases, OA concentration remains similar after the different UV-exposures, with no statistically significant differences regarding the UV source ($p = 0.8677$) or water matrix ($p = 0.7460$), indicating that under the tested conditions, no appreciable photodegradation occurred. The maximum observed degradation was 12.5 % (SD ± 6.3 %), confirming the high resistance of OA to UV photodegradation.

The high stability of OA under natural sunlight and UV-A exposure has been reported (Camacho-Muñoz et al., 2020; Pan et al., 2020; Qiu

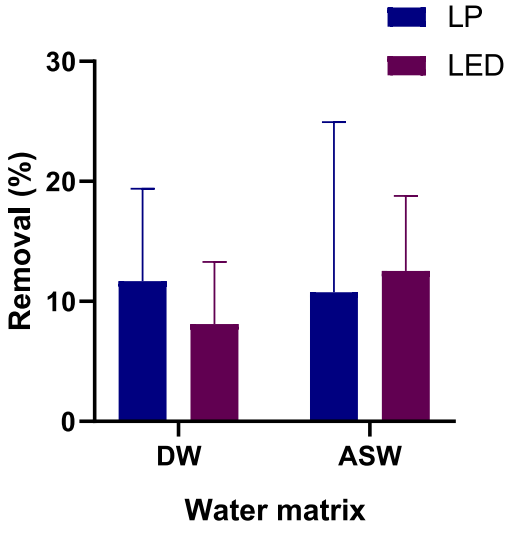

Fig. 1. Photo-degradation percentage of okadaic acid in distilled water (DW) and artificial seawater (ASW) under two different UV-sources: LP-Hg and UV-LED. Experimental conditions: UV exposure: 180 min. Mean irradiance: 0.378 ± 0.091 mW·cm^{-2} (LP-Hg); 0.072 ± 0.005 mW·cm^{-2} (UV-LED). Data represent mean values ± standard deviation (SD) of three independent replicates ($n = 3$).

et al., 2025), while noticeable degradation has only been observed under high-intensity sources, such as a 1000 W polychromatic high-pressure mercury lamp (Pan et al., 2020; Qiu et al., 2025), suggesting that much higher energy doses or broader wavelength spectra are required compared to the 10 W lamps used in our study. Similarly, Murray et al., 2018, demonstrated that high-intensity pulsed polychromatic light could reduce OA toxicity in *Daphnia pulex*, further emphasizing the role of light intensity and spectrum in treatment effectiveness.

In our study, the maximum monochromatic UV dose applied was 4.08 J/cm^2, which is already relevant for industrial applications, yet insufficient to induce substantial OA photodegradation. These results highlight the limitations of direct UV photolysis and reinforce the need to explore advanced photochemical techniques for effective OA removal in marine environments.

3.2. Photo-chemical degradation

To identify effective OA removal strategies, various photochemical processes were tested using two UV sources (LP-Hg and UV-LED) in distilled (DW) and artificial seawater (ASW). Three different reagents, namely hydrogen peroxide (HP), sodium peroxydisulfate (PDS) and potassium peroxymonosulfate (PMS) were applied as a source of potential reactive oxygen or sulfate species. The OA degradation profiles are depicted in Fig. 2.

As illustrated in Fig. 2, photochemical processes can degrade OA with high effectiveness than photolytic process alone. High efficacy is obtained in DW, for which the three processes are able to degrade >90 % of OA within 120 min of exposure to either LP-Hg or UV-LED (Fig. 2), although an exception is observed in the case of UV-LED/HP, where the maximum OA degradation account for 79.12 % (S.D. ± 0.55). In ASW, the process is slowed down in the case of UV/HP (H_2O_2; Fig. 2 a-b) and UV/PDS ($S_2O_8^{2-}$; Fig. 2 c-d). Interestingly, in the case of UV/PMS (HSO_5^-; Fig. 2 e-f), the degradation of OA is greatly enhanced under both UV sources in ASW.

OA degradation followed pseudo-first-order kinetics, allowing calculation of the rate constant k_{obs} (min^{-1}) to evaluate the performance of each UV source and reagent (Fig. 3). OA degradation profiles fitted to a pseudo-first-order model (Eq. (1)) are shown in Fig. S2 (Supplementary Material), while the corresponding kinetic parameters are summarized in Table S1.

According to the results represented in Fig. 3, the photo-chemical processes follows a general trend for the OA degradation, which is UV/PMS > UV/PDS > UV/HP, with same trend observed when irradiation source is LP-Hg or UV-LED but differences are more evidenced under UV LP-Hg, assuming that the molar absorption coefficient by the different reagents is favoured at the lowest wavelength, i.e. 254 nm (LP-Hg) (Tang et al., 2023).

In distilled water (DW), k_{obs} values consistently increased in the order of HP < PDS < PMS, with a 43.8–82.7 % increase from HP to PDS and a 76.5–79.5 % increase from HP to PMS. Nonetheless, no significant differences were observed among these three photo-chemical processes in DW under both UV sources ($p > 0.9$). In artificial seawater (ASW), the k_{obs} values exhibited the same trend, highlighting the significant increase in k_{obs} for PMS processes, which became statistically significant when compared with HP or PDS under LP-Hg ($p < 0.01$) and UV-LED ($p < 0.001$).

When comparing the different water matrices (DW vs. ASW), the k_{obs} values showed a decrease of 72.8–89.9 % for HP and a decrease of 67.8–76.6 % for PDS, confirming that salinity negatively interferes with these two photo-chemical processes, being the hydroxyl radical-based process (HP) more affected than persulfate-based process. On the other hand, k_{obs} significantly increased in PMS processes, indicating a positive interference of salinity that greatly enhances the degradation rate of OA in ASW. This highlights the distinct behavior of reaction kinetics in different water environments. The results obtained for degradation kinetics align with the reagent consumption profiles (Fig. S3).

The distinct degradation levels observed for OA over time may be attributed to the different mechanisms of action inherent to the photochemical processes examined. The photolysis of HP primarily generates •OH in the initial step, as illustrated by Eq. (2). These radicals are highly reactive and non-selective, enabling them to rapidly interact with a broad spectrum of organic compounds in water, effectively degrading OA in systems devoid of other water matrix components (Fig. 2; Fig. 3). However, in the presence of dissolved salts, the efficiency of this process appears to decrease significantly. This reduction may be due to the scavenging of •OH radicals by salts through competitive reactions, leading to the formation of halogen radical species, which subsequently propagate and reduce the overall degradation capacity.

$$H_2O_2 + h\nu \rightarrow \bullet OH + \bullet OH \ (\Phi = 1.0) \quad (2)$$

$$S_2O_8^{2-} + h\nu \rightarrow SO_4^{\bullet -} + SO_4^{\bullet -} \ (\Phi = 1.8) \quad (3)$$

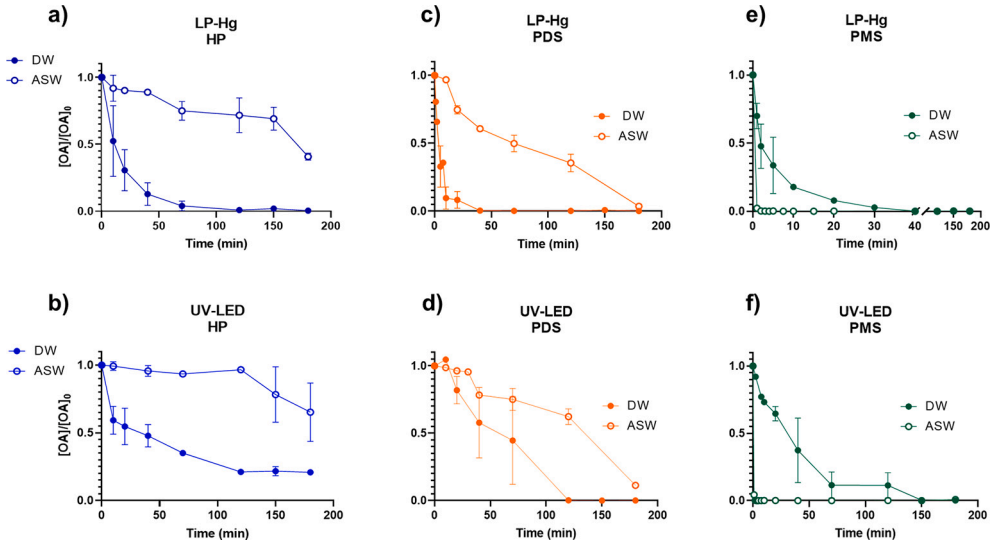

Fig. 2. Degradation profiles of okadaic acid in distilled water (DW) and artificial seawater (ASW), according to the UV source: LP-Hg or UV-LED and reagent: hydrogen peroxide (HP), sodium peroxydysulfate (PDS) or potassium peroxymonosulfate (PMS). Experimental conditions: Mean irradiance: 0.378 ± 0.091 mW·cm^{-2} (LP-Hg); 0.072 ± 0.005 mW·cm^{-2} (UV-LED). [H_2O_2]; [$S_2O_8^{2-}$]; [HSO_5^-] = 0.5 mM). Data represent mean values ± standard deviation (SD) of three independent replicates (n = 3). DL = 2 ng OA/mL.

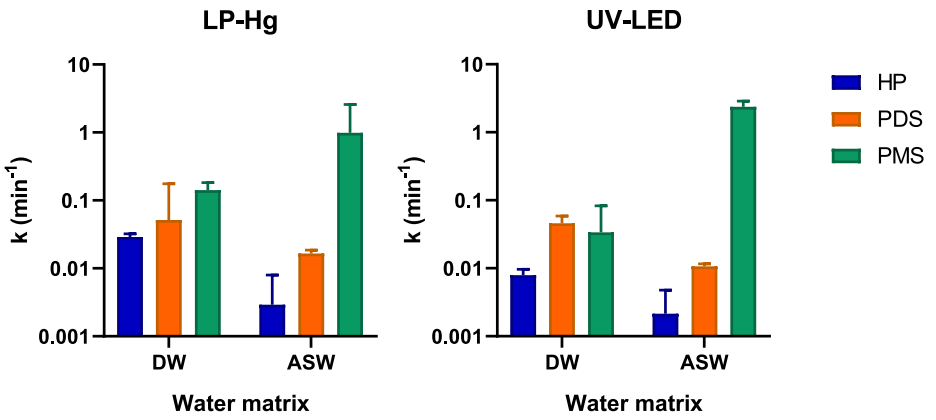

Fig. 3. Time-based kinetic rate constant of okadaic acid photodegradation in DW and ASW, with the presence of hydrogen peroxide (HP), sodium peroxydisulfate (PDS) or potassium peroxymonosulfate (PMS) under two different UV-sources: LP-Hg or UV-LED. Experimental conditions: Mean irradiance: 0.378 ± 0.091 mW·cm^{-2} (LP-Hg); 0.072 ± 0.005 mW·cm^{-2} (UV-LED). [H_2O_2]; [$S_2O_8^{2-}$]; [HSO_5^-] = 0.5 mM). Data represent mean values ±95 % CI.

$$HSO_5^- + h\nu \rightarrow SO_4^{\bullet -} + \bullet OH \ (\Phi = 1.04) \quad (4)$$

In sulfate-based processes, sulfate radicals ($SO_4^{\bullet -}$) are generated via the photolysis of PDS, as represented by Eq. (3). Sulfate radicals are recognized for their higher selectivity towards electron-rich organic compounds (Lee et al., 2020; Nihemaiti et al., 2018), which may explain the slightly enhanced degradation of OA observed in comparison with hydroxyl radical-based processes, under both UV sources (Fig. 3). In this regard, the unique ability of $SO_4^{\bullet -}$ to induce decarboxylation reactions is particularly relevant (Lee et al., 2020), as OA possess carboxylic acid groups that are susceptible to this mechanism (Pan et al., 2020). Additionally, similar decarboxylation processes have been observed in aromatic carboxylic acids under sulfate radical attack, which further supports the likelihood of this degradation pathway for OA (Lee et al., 2020). Along with the carboxyl groups, the ether and hydroxyl groups in OA represent other electron-rich sites prone to oxidative attack by $SO_4^{\bullet -}$, enhancing the overall degradation efficiency.

Similarly to •OH, $SO_4^{\bullet -}$ also reacts with dissolved salts, leading to the formation of reactive halogen species through propagation reactions, which in turn diminishes degradation efficiency in ASW (Fig. 3). Nevertheless, the interference observed appears to be less significant compared to HP, as the degradation of OA in ASW is more efficient with PDS than with HP. The higher selectivity above discussed of $SO_4^{\bullet -}$ may play a crucial role in this context by allowing more targeted reactions with OA despite the presence of competitive species in the water matrix. For instance, major ions in seawater, such as chlorides, react more rapidly with •OH ($k = 4.3 \cdot 10^9$ $M^{-1} \cdot s^{-1}$) than with $SO_4^{\bullet -}$ ($k = 3.1 \cdot 10^8$ $M^{-1} \cdot s^{-1}$) (Lee et al., 2020). A similar trend is observed with bromides, another relevant halide in seawater ($k_{\bullet OH\text{-}Br^-} = 1.1 \cdot 10^{10}$ $M^{-1} \cdot s^{-1}$; $k_{SO4\bullet -\text{-}Br^-} = 3.5 \cdot 10^9$ $M^{-1} \cdot s^{-1}$) (Matthew and Anastasio, 2006; Redpath and Willson, 1975). This selectivity may help mitigate the negative effects typically observed with hydroxyl radicals in saline environments.

In the case of PMS, both •OH and $SO_4^{\bullet -}$ can be generated initially (Eq. (4)). However, the reactivity of PMS with chloride ions to form chlorine species ($2Cl^- + HSO_5^- + H^+ \rightarrow HSO_4^{2-} + Cl_2 + OH^-$; $k = 32.5$ $M^{-1} \cdot s^{-1}$; $Cl^- + HSO_5^- \rightarrow HClO + SO_4^{2-}$; $k = 6.5 \cdot 10^{-4}$ $M^{-1} \cdot s^{-1}$) could significantly enhance the overall degradation efficacy (Song et al., 2024), as it is observed on Fig. 3. Previous studies have shown that the formation of free chlorine species in PMS/Cl^- system is effective against microorganisms and organic pollutants (Song et al., 2024). Thus, the formation of reactive chlorine species (RCS) in this system could further participate in the degradation of OA. In fact, the presence of chlorine, which has been documented in prior studies (Guerra-Rodríguez et al., 2022), is also prone to photolysis under both UV sources, further contributing to OA degradation. At the basic pH of ASW, hypochlorite ions (OCl^-) are the dominant species and exhibit a strong absorption peak at 292 nm (ε = 365 ± 8 $M^{-1} \cdot cm^{-1}$) (Yin et al., 2018). Unlike hydrogen peroxide (HP), which requires shorter wavelengths for activation, OCl^- can be efficiently activated by longer-wavelength UV light, such as that emitted by UV-LEDs, potentially explaining the rapid degradation observed in ASW (Pizzichetti et al., 2023). Therefore, the combined high reactivity of PMS and Cl^- in the system, along with the UV absorption properties of the formed OCl^- species, may explain the enhanced OA degradation observed in ASW with UV/PMS treatment.

Most photochemical degradation studies have focused on freshwater toxins, with limited research on marine biotoxins. For instance, He et al. (2013) evaluated the same three photochemical processes studied here for degrading the cyanotoxin cylindrospermopsin, reporting higher removal with persulfate-based systems compared to HP. They also found that radical scavengers in tap water reduced UV/HP efficiency, while persulfate systems were less affected, supporting our findings. Similarly, Khan et al. (2014), observed greater atrazine degradation with sulfate radicals than with hydroxyl radicals under comparable conditions.

Literature on marine biotoxin degradation remains scarce. Camacho-Muñoz et al. (2020) reported the only study using UV/TiO_2 against OA, showing a five-fold decrease in degradation rate in seawater. This aligns with our findings for UV/HP, reinforcing that hydroxyl radicals are more susceptible to scavenging by dissolved salts under saline conditions.

3.3. Transformation products (TPs)

To gain information on the OA-TPs present in distilled water persulfate-based processes samples, we analyzed them in a full spectrum scanning in positive and negative ion modes. Analysis of HP-based processes was excluded due to their lower observed degradation rate constant in previous sections, allowing us to focus on persulfate-based processes for optimized analysis.

The OA and TPs identification was performed according to Section 2.4.2. and Text S3. Although the optimal mode for OA-TP detection remains uncertain, better sensitivity is generally achieved in ESI^- using the deprotonated ion $[M - H]^-$. In our study, only the OA ion (*m/z* 805.477 $[M + H]^+$) was detected in positive mode, while negative mode $[M - H]^-$ enabled identification of both OA (*m/z* 803.459) and a known transformation product (*m/z* 757.453), suggesting ESI^- as the more sensitive approach. The identification of this TP, associated with norokadanone, was further confirmed by its accurate isotopic pattern and fragmentation spectra (Fig. S4), consistent with previously reported data (Camacho-Muñoz et al., 2020; Pan et al., 2020).

The concentration of the detected OA-TP (*m/z* 757.453 [M - H]-) in the PDS treatment with LP-Hg appeared to decrease over time (from 0 to 30 min) and fell below the limit of quantification (< LOQ) after 45 min (Table 2). In contrast, no consistent trend in OA-TP concentration

changes was observed in the UV-LED PDS treatment and the two PMS treatments (Table 2). Notably, Camacho-Muñoz et al. (2020), identified this OA-TP as the only transformation product detected, while Pan et al. (2020) reported it as the most abundant among the OA-derived products. In both studies, a time-dependent decrease in this OA-TP was observed. Pan et al. (2020) detected it at higher concentrations within the first 20 min, after which levels rapidly declined. Camacho-Muñoz et al. (2020) detected higher concentrations at 2.5 min, with this OA-TP becoming undetectable after 10 min. The transformation of OA into this OA-TP seems to occur very quickly, as the OA-TP was detected at the measured 0 min in the current study; and then transformed into another unknown OA-TP. It is crucial to note that the detected OA-TP was absent from the standard solution, i.e. OA Certified Reference Material (CRM) (See Text S3), and the initial standard used to prepare the samples, i.e. OA potassium salt.

3.4. Final toxicity: PP2A activity

The detoxification of aqueous samples containing OA was evaluated under various photochemical treatments (HP, PDS, and PMS) using two UV light sources (UV-LED and LP-Hg) in both DW and ASW. Tests with HP were included despite its lower k_{obs} values, as they allow corroboration of final toxicity. Detoxification efficiency was assessed through PP2A activity measurements, with higher PP2A activity percentages indicating greater detoxification (i.e., degradation of OA into lower toxicity transformation products). Results are presented as the percentage of PP2A activity in Fig. 4. Notably, the highest toxicity was observed at the start of the experiment, coinciding with OA maximum concentration.

The detoxification efficacy of aqueous samples containing OA varied across photochemical treatments, UV light sources, and water matrices. Among the treatments, PDS consistently demonstrated the highest detoxification in distilled water, particularly under LP-Hg, where PP2A activity reached approximately 85 % within 60 min. PMS, although with similar results than PDS in distilled water (reaching about 80 % PP2A activity), showed remarkable performance in ASW. Under UV-LED exposure in ASW, PMS process achieved nearly complete detoxification, with PP2A activity approaching 99 % within just 15 min. This suggests that PMS is highly effective in saline environments, possibly due to the generation of additional reactive species like chlorine radicals, which may enhance OA degradation, as explained in Section 3.2. Conversely, HP demonstrated minimal effectiveness under all conditions, with PP2A activity consistently ranging between 15 and 25 % in ASW regardless of the UV source, aligning with the observed trends in OA degradation (Section 3.2). This low performance was particularly pronounced in complex matrices like seawater.

The marked contrast between PDS and PMS in seawater highlights the importance of water matrix in influencing detoxification efficiency. PDS remained more effective in distilled water, likely due to fewer competing ions, whereas PMS outperformed in saline environments under UV-LED, achieving rapid and near-total detoxification. These findings suggest that PMS may be particularly suitable for applications in marine settings, while PDS could be preferred in simpler, distilled water matrices. The poor performance of HP across all conditions indicates it may be unsuitable as a primary agent for OA detoxification in similar scenarios.

Photochemical processes, specially persulfate-based processes, appear highly effective in reducing OA initial toxicity, as evidenced by the rapid decrease in toxicity (Fig. 4). This detoxification aligns with previous research showing up to 88 % toxicity reduction in OA solutions following photodegradation (Murray et al., 2018). The increase in PP2A activity observed in this study confirms not only the effective degradation of OA across photochemical treatments but also suggests that the OA-TP formed, exhibit significantly lower toxicity compared to the original compound. Norokadanone, identified as TP *m/z* 757.453 [M-H]-, was detected as the primary TP, consistent with previous findings by Camacho-Muñoz et al. (2020). This transformation is attributed to the decarboxylation of OA, indicating that the carboxyl functional group plays a critical role in its diarrhetic toxicity (Lassila et al., 2015). The removal of this group correlates with a marked reduction in toxicity, as also reported in similar studies (Camacho-Muñoz et al., 2020; Pan et al., 2020).

Table 2
Mean concentration (ng/mL) of okadaic acid and transformation product (*m/z* 757.453 [M - H]-), as determined by LC-HRMS.

PDS			PMS		
Exposure Time (min.)	[OA] ng/mL	[TP] ng/mL	Exposure Time (min.)	[OA] ng/mL	[TP] ng/mL
		LP-Hg			
0	21.21	1.47	0	19.16	1.06
1	17.24	1.79	1	9.73	0.07
2	13.93	1.71	2	5.84	0.94
5	10.78	1.51	5	0.18	0.93
7.5	6.58	1.62	7.5	–	0.36
10	5.34	1.19	10	–	0.42
20	2.82	0.43	20	–	1.2
30	0.94	0.29	30	–	0.74
		UV-LED			
0	19.13	0.65	0	19.95	0.43
5	18.7	0.56	2.5	24.34	1.82
10	17.21	0.29	5	15.48	1.08
30	12.13	0.78	7.5	13.68	1.54
45	12.58	0.37	10	12.51	0.91
60	10.51	0.35	20	12.5	0.97
			30	9.1	0.35
			45	5.28	1.58
			60	3.15	0.88

4. Conclusions

The present study demonstrates that UV-assisted photochemical processes can effectively degrade and detoxify okadaic acid (OA), with performance influenced by the type of oxidant, UV source, and water matrix. Among the reagents tested, PMS was the most effective, particularly in artificial seawater (ASW), where salinity significantly enhanced its degradation capacity. In contrast, PDS performed best in distilled water (DW), while HP showed the lowest efficacy, especially in saline matrices and under UV-LED.

The observed degradation rate constants (k_{obs}) followed a consistent trend: UV/PMS > UV/PDS > UV/HP, with differences more pronounced under LP-Hg irradiation. In ASW, UV/PMS showed significantly higher k_{obs} values, while salinity inhibited HP and PDS by up to 89.9 % and 76.6 %, respectively. Both UV sources supported OA degradation, with UV-LED performing comparably to LP-Hg in ASW when combined with PMS.

Norokadanone (*m/z* 757.453), the main transformation product, was formed via decarboxylation and exhibited significantly lower toxicity. Detoxification was confirmed through PP2A activity recovery above 98 % for UV/PMS in ASW, in contrast to 18.8–20.2 % for HP and 35.7–80.3 % for PDS under similar conditions.

Overall, persulfate-based processes, especially UV/PMS, are promising for OA removal in marine environments. However, performance is matrix-dependent: while salinity enhances PMS activity, it hinders PDS. These findings highlight the importance of considering water chemistry when selecting photochemical treatments.

Future studies should investigate the behavior of these processes in natural seawater and real-world scenarios, including potential by-products and long-term toxicity, as well as their performance in continuous-flow reactors, where photochemical efficiency may differ from batch systems, to support the development of safe and scalable treatment strategies for marine biotoxins.

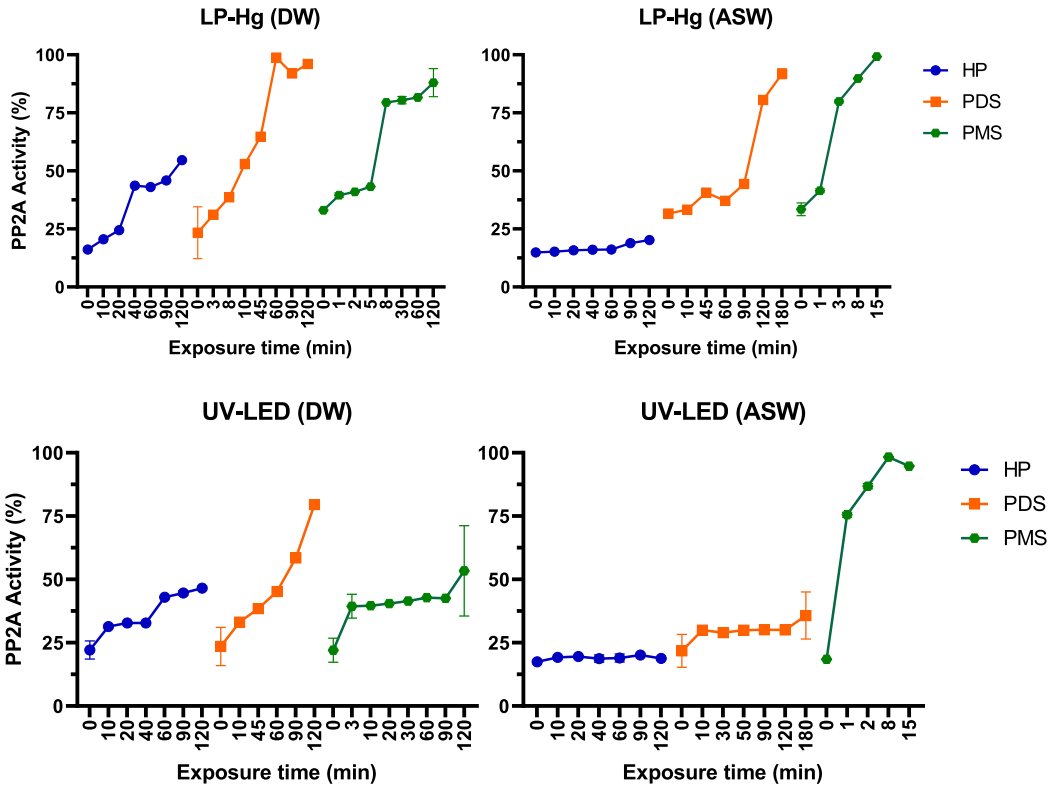

Fig. 4. Toxicity profile (in terms of PP2A activity, %) after Okadaic Acid photodegradation in DW and ASW with the presence of Hydrogen Peroxide (HP), Sodium peroxodysulfate (PDS) or Potassium peroxymonosulfate (PMS) under two different UV-sources: LP-Hg or LED.

CRediT authorship contribution statement

Javier Moreno-Andrés: Writing – review & editing, Writing – original draft, Visualization, Resources, Project administration, Methodology, Investigation, Funding acquisition, Conceptualization. **Sandra Lage:** Writing – review & editing, Writing – original draft, Supervision, Resources, Methodology, Investigation, Formal analysis, Conceptualization. **Ana Catarina Braga:** Writing – review & editing, Resources, Methodology, Investigation. **Pedro Reis Costa:** Writing – review & editing, Writing – original draft, Visualization, Supervision, Resources, Project administration, Methodology, Investigation, Funding acquisition, Conceptualization.

Declaration of competing interest

The authors declare that they have no known competing financial interests or personal relationships that could have appeared to influence the work reported in this paper.

Acknowledgments

Authors would like to acknowledge the financial support through the project MOBILED: PCM_00015 funded by the Department of University, Research and Innovation of the Regional Government of Andalusia (Spain) and by the European Union NextGenerationEU/PRTR C.17, I1. Authors also wants to acknowledge the financial support of the project ECOTRANSEAS (TED2021–130994B-C31) funded by MCIN/AEI/10.13039/501100011033 and by the European Union NextGenerationEU/PRTR. JM acknowledges the funding received from the Ministry of Science, Innovation, and Universities for mobility stays of professors and researchers, under the "José Castillejo" program. Ref.: CAS21/00228. SL was supported by "la Caixa" Foundation (ID 100010434) through a Junior Leader Retaining Fellowship (LCF/BQ/PR23/11980049), and Portuguese national funds from FCT—Foundation for Science and Technology through projects UIDB/04326/2020, UIDP/04326/2020, and LA/P/0101/2020; the operational programs CRESC Algarve 2020 and COMPETE 2020 through project EMBRC.PT ALG-01-0145-FEDER-022121.

Appendix A. Supplementary data

Supplementary data to this article can be found online at https://doi.org/10.1016/j.marpolbul.2025.118183.

Data availability

Data will be made available on request.

References

Alexander, J., Benford, D., Boobis, A., Ceccatelli, S., Cravedi, J., Di Domenico, A., Doerge, D., Dogliotti, E., Edler, L., Farmer, P., Fink-gremmels, J., Fürst, P., Guerin, T., Knutsen, H.K., Livesey, C., Machala, M., Mutti, A., Schlatter, J., Van Leeuwen, R., 2009. Scientific opinion of the panel on contaminants in the food chain on a request from the European Commission on marine biotoxins in shellfish – summary on regulated marine biotoxins. EFSA Journal 1306, 1–23.

Bian, Y., Feng, X., song, Zhang, Y., Du, C., Wen, Y. qing, 2024. Marine toxins in environment: recent updates on depuration techniques. Ecotoxicol. Environ. Saf. 284, 116990. https://doi.org/10.1016/J.ECOENV.2024.116990.

Blanco, J., Martín-Morales, E., Álvarez, G., 2018. Stability of okadaic acid and 13-desmethyl spirolide C in seawater and sediment. Mar. Chem. 207, 21–25. https://doi.org/10.1016/J.MARCHEM.2018.10.007.

Bolton, J.R., Linden, K.G., 2003. Standardization of methods for fluence (UV dose) determination in bench-scale UV experiments. J. Environ. Eng. 129, 209–215. https://doi.org/10.1061/(ASCE)0733-9372(2003)129:3(209).

Bosch-Orea, C., Sanchís, J., Farré, M., Barceló, D., 2017. Analysis of lipophilic marine biotoxins by liquid chromatography coupled with high-resolution mass spectrometry in seawater from the Catalan Coast. Anal. Bioanal. Chem. 409, 5451–5462. https://doi.org/10.1007/S00216-017-0536-Y.

Braga, A.C., Rodrigues, S.M., Lourenço, H.M., Costa, P.R., Pedro, S., 2023. Bivalve shellfish safety in Portugal: variability of faecal levels, metal contaminants and marine biotoxins during the last decade (2011−2020). Toxins (Basel) 15, 91. https://doi.org/10.3390/TOXINS15020091.

Camacho-Muñoz, D., Lawton, L.A., Edwards, C., 2020. Degradation of okadaic acid in seawater by UV/TiO2 photocatalysis – proof of concept. Sci. Total Environ. 733, 139346. https://doi.org/10.1016/J.SCITOTENV.2020.139346.

Costa, P.R., Moita, T., Rodrigues, S.M., 2014. Estimating the contribution of N-sulfocarbamoyl paralytic shellfish toxin analogs GTX6 and C3 + 4 to the toxicity of mussels (Mytilus galloprovincialis) over a bloom of Gymnodinium catenatum. Harmful Algae 31, 35–40. https://doi.org/10.1016/J.HAL.2013.09.009.

Costa, P.R., Costa, S.T., Braga, A.C., Rodrigues, S.M., Vale, P., 2017. Relevance and challenges in monitoring marine biotoxins in non-bivalve vectors. Food Control 76, 24–33. https://doi.org/10.1016/J.FOODCONT.2016.12.038.

Costa, S.T., Rudnitskaya, A., Vale, C., Guilhermino, L., Botelho, M.J., 2020. Sorption of okadaic acid lipophilic toxin onto plastics in seawater. Mar. Pollut. Bull. 157, 111322. https://doi.org/10.1016/J.MARPOLBUL.2020.111322.

Costa, C.Q.V., Afonso, I.I., Lage, S., Costa, P.R., Canário, A.V.M., Da Silva, J.P., 2022. Quantitation overcoming matrix effects of lipophilic toxins in Mytilus galloprovincialis by liquid chromatography-full scan high resolution mass spectrometry analysis (LC-HR-MS). Mar. Drugs 20, 143. https://doi.org/10.3390/MD20020143/S1.

Dias, M., Özkan, B., Ramos, J., Marques, A., Rosa, R., Costa, P.R., Maulvault, A.L., 2025. Hot and toxic: accumulation dynamics and ecotoxicological responses of mussel Mytilus galloprovincialis exposed to marine biotoxins during a marine heatwave. Mar. Pollut. Bull. 213, 117629. https://doi.org/10.1016/J.MARPOLBUL.2025.117629.

FAO, 2008. Bivalve depuration: Fundamental and practical aspects, FAO Fisher. ed. Food and Agriculture Organization of the United Nations (FAO), Rome.

Fernández, R., Mamán, L., Jaén, D., Fuentes, L.F., Ocaña, M.A., Gordillo, M.M., 2019. Dinophysis species and diarrhetic shellfish toxins: 20 years of monitoring program in Andalusia, South of Spain. Toxins 11, 189. https://doi.org/10.3390/TOXINS11040189.

González-Jartín, J.M., de Castro Alves, L., Alfonso, A., Piñeiro, Y., Vilar, S.Y., Rodríguez, I., Gomez, M.G., Osorio, Z.V., Sainz, M.J., Vieytes, M.R., Rivas, J., Botana, L.M., 2020. Magnetic nanostructures for marine and freshwater toxins removal. Chemosphere 256, 127019. https://doi.org/10.1016/j.chemosphere.2020.127019.

Guerra-Rodríguez, S., Rodríguez, E., Moreno-Andrés, J., Rodríguez-Chueca, J., 2022. Effect of the water matrix and reactor configuration on Enterococcus sp. inactivation by UV-A activated PMS or H2O2. J. Water Process Eng. 47, 102740. https://doi.org/10.1016/J.JWPE.2022.102740.

He, X., De La Cruz, A.A., Dionysiou, D.D., 2013. Destruction of cyanobacterial toxin cylindrospermopsin by hydroxyl radicals and sulfate radicals using UV-254 nm activation of hydrogen peroxide, persulfate and peroxymonosulfate. J. Photochem. Photobiol. A Chem. 251, 160–166. https://doi.org/10.1016/j.jphotochem.2012.09.017.

Henigman, U., Mozetič, P., Francé, J., Knific, T., Vadnjal, S., Dolenc, J., Kirbiš, A., Biasizzo, M., 2024. Okadaic acid as a major problem for the seafood safety (Mytilus galloprovincialis) and the dynamics of toxic phytoplankton in the Slovenian coastal sea (Gulf of Trieste, Adriatic Sea). Harmful Algae 135, 102632. https://doi.org/10.1016/J.HAL.2024.102632.

Khan, J.A., He, X., Shah, N.S., Khan, H.M., Hapeshi, E., Fatta-Kassinos, D., Dionysiou, D. D., 2014. Kinetic and mechanism investigation on the photochemical degradation of atrazine with activated H2O2, S2O82-and HSO5. Chem. Eng. J. 252, 393–403. https://doi.org/10.1016/j.cej.2014.04.104.

Kim, Y., Choi, P.J., Jang, A., 2024. Effect of NaOCl and ClO2 on seawater desalination using reverse osmosis with cartridge filtration as the pretreatment during the algal bloom. Chemosphere 349, 140944. https://doi.org/10.1016/J.CHEMOSPHERE.2023.140944.

Lassila, T., Hokkanen, J., Aatsinki, S.M., Mattila, S., Turpeinen, M., Tolonen, A., 2015. Toxicity of carboxylic acid-containing drugs: the role of acyl migration and CoA conjugation investigated. Chem. Res. Toxicol. 28, 2292–2303. https://doi.org/10.1021/acs.chemrestox.5b00315.

Lee, H., Lim, J., Zhan, M., Hong, S., 2019. UV-LED/PMS preoxidation to control fouling caused by harmful marine algae in the UF pretreatment of seawater desalination. Desalination 467, 219–228. https://doi.org/10.1016/J.DESAL.2019.06.009.

Lee, J., Von Gunten, U., Kim, J.H., 2020. Persulfate-based advanced oxidation: critical assessment of opportunities and roadblocks. Environ. Sci. Technol. https://doi.org/10.1021/acs.est.9b07082.

Levchuk, I., Homola, T., Moreno-Andrés, J., Rueda-márquez, J.J., Dzik, P., Ángel, M., Sillanpää, M., Manzano, M.A., Vahala, R., 2019. Solar photocatalytic disinfection using ink-jet printed composite TiO2/SiO2 thin films on flexible substrate: applicability to drinking and marine water. Sol. Energy 191, 518–529. https://doi.org/10.1016/j.solener.2019.09.038.

Li, J., Ruan, Y., Mak, Y.L., Zhang, X., Lam, J.C.W., Leung, K.M.Y., Lam, P.K.S., 2021. Occurrence and Trophodynamics of marine lipophilic phycotoxins in a subtropical marine food web. Environ. Sci. Technol. 55, 8829–8838. https://doi.org/10.1021/ACS.EST.1C01812.

Li, D., Qiu, J., Wang, X., Li, A., Wu, G., Yin, C., Yang, Y., 2024. Spatial distribution of lipophilic shellfish toxins in seawater and sediment in the Bohai Sea and the Yellow Sea, China. Chemosphere 362, 142780. https://doi.org/10.1016/j.chemosphere.2024.142780.

Liang, C., Huang, C.F., Mohanty, N., Kurakalva, R.M., 2008. A rapid spectrophotometric determination of persulfate anion in ISCO. Chemosphere 73, 1540–1543. https://doi.org/10.1016/j.chemosphere.2008.08.043.

Martinez-Albores, Lopez-Santamarina, Rodriguez, Ibarra, del Carmen Mondragón, Miranda, Lamas, Cepeda, 2020. Complementary methods to improve the depuration of bivalves: a review. Foods 9 (129). https://doi.org/10.3390/foods9020129.

Martín-Sómer, M., Pablos, C., Adán, C., van Grieken, R., Marugán, J., 2023. A review on LED technology in water photodisinfection. Sci. Total Environ. 885, 163963. https://doi.org/10.1016/J.SCITOTENV.2023.163963.

Matthew, B.M., Anastasio, C., 2006. A chemical probe technique for the determination of reactive halogen species in aqueous solution: part 1 - bromide solutions. Atmos. Chem. Phys. 6, 2423–2437. https://doi.org/10.5194/ACP-6-2423-2006.

Moreno-Andrés, J., Acevedo-Merino, A., Nebot, E., 2018. Study of marine bacteria inactivation by photochemical processes: disinfection kinetics and growth modeling after treatment. Environ. Sci. Pollut. Res. 25, 27693–27703. https://doi.org/10.1007/s11356-017-1185-6.

Moreno-Andrés, J., Tierno-Galán, M., Romero-Martínez, L., Acevedo-Merino, A., Nebot, E., 2023. Inactivation of the waterborne marine pathogen *Vibrio alginolyticus* by photo-chemical processes driven by UV-A, UV-B, or UV-C LED combined with H_2O_2 or HSO_5. Water Res. 232, 119686. https://doi.org/10.1016/J.WATRES.2023.119686.

Murray, I.M.T., Rowan, N.J., McNamee, S., Campbell, K., Fogarty, A.M., 2018. Pulsed light reduces the toxicity of the algal toxin okadaic acid to freshwater crustacean Daphnia pulex. Environ. Sci. Pollut. Res. 25, 607–614. https://doi.org/10.1007/S11356-017-0472-6.

Nihemaiti, M., Miklos, D.B., Hübner, U., Linden, K.G., Drewes, J.E., Croué, J.P., 2018. Removal of trace organic chemicals in wastewater effluent by UV/H_2O_2 and UV/PDS. Water Res. 145, 487–497. https://doi.org/10.1016/j.watres.2018.08.052.

Pan, L., Chen, J., He, X., Zhan, T., Shen, H., 2020. Aqueous photodegradation of okadaic acid and dinophysistoxin-1: persistence, kinetics, photoproducts, pathways, and toxicity evaluation. Sci. Total Environ. 743, 140593. https://doi.org/10.1016/j.scitotenv.2020.140593.

Pepe-Vargas, P., Castro, L.R., Alves-de-Souza, C., Llanos-Rivera, A., 2024. Effects of the harmful algal bloom toxin, okadaic acid, on the mechanoreceptors of larval anchoveta (*Engraulis ringens*) under varying environmental conditions. Front. Mar. Sci. 11, 1446509. https://doi.org/10.3389/FMARS.2024.1446509. /BIBTEX.

Pizzichetti, R., Reynolds, K., Pablos, C., Casado, C., Moore, E., Stanley, S., Marugán, J., 2023. Removal of diclofenac by UV-B and UV-C light-emitting diodes (LEDs) driven advanced oxidation processes (AOPs): wavelength dependence, kinetic modelling and energy consumption. Chem. Eng. J. 471, 144520. https://doi.org/10.1016/J.CEJ.2023.144520.

Porcar-Santos, O., Cruz-Alcalde, A., López-Vinent, N., Zanganas, D., Sans, C., 2020. Photocatalytic degradation of sulfamethoxazole using TiO2 in simulated seawater: evidence for direct formation of reactive halogen species and halogenated by-products. Sci. Total Environ. 736, 139605. https://doi.org/10.1016/j.scitotenv.2020.139605.

Pousty, D., Mamane, H., Cohen-Yaniv, V., Bolton, J.R., 2022. Ultraviolet actinometry – determination of the incident photon flux and quantum yields for photochemical systems using low-pressure and ultraviolet light-emitting diode light sources. J. Environ. Chem. Eng. 10, 107947. https://doi.org/10.1016/j.jece.2022.107947.

Qiu, J., Yin, C., Li, A., Yang, Y., Wang, G., Li, D., 2025. Effects of microorganisms, temperature and irradiation on the stability of dissolved okadaic acid and dinophysistoxin-1 in seawater. Mar. Environ. Res. 204, 106969. https://doi.org/10.1016/J.MARENVRES.2025.106969.

Reboreda, A., Lago, J., Chapela, M.J., Vieites, J.M., Botana, L.M., Alfonso, A., Cabado, A. G., 2010. Decrease of marine toxin content in bivalves by industrial processes. Toxicon 55, 235–243. https://doi.org/10.1016/J.TOXICON.2009.07.029.

Redpath, J.L., Willson, R.L., 1975. Chain reactions and radiosensitization: model enzyme studies. Int. J. Radiat. Biol. Relat. Stud. Phys., Chem. Med. 27, 389–398. https://doi.org/10.1080/09553007514550361.

Rodríguez, L.P., González, V., Martínez, A., Paz, B., Lago, J., Cordeiro, V., Blanco, L., Vieites, J.M., Cabado, A.G., 2015. Occurrence of lipophilic marine toxins in shellfish from Galicia (NW of Spain) and synergies among them. Mar. Drugs 13, 1666–1687. https://doi.org/10.3390/MD13041666.

Sha, H., Su, X., Zhou, P., 2024. UV/H2O2 and UV/PDS treatment of an emerging cyanotoxin (aerucyclamide A): kinetics, transformation products, and toxicity. Chem. Eng. J. 483, 149353. https://doi.org/10.1016/J.CEJ.2024.149353.

Sheng, C., He, X., Chen, J., Fan, S., Li, X., 2025. Seasonal dynamics of lipophilic marine algal toxins in water body and sediment environments of nearshore mariculture areas in northern China. Mar. Pollut. Bull. 215, 117920. https://doi.org/10.1016/J.MARPOLBUL.2025.117920.

Song, Z., Zhang, Y., Yang, Y., Chen, Y., Ren, N., Duan, X., 2024. Kinetics and mechanisms of non-radically and radically induced degradation of bisphenol A in a peroxymonosulfate-chloride system. Environ. Sci. Ecotechnol. 22, 100452. https://doi.org/10.1016/J.ESE.2024.100452.

Tang, L., Li, A., Kong, M., Dionysiou, D.D., Duan, X., 2023. Effects of wavelength on the treatment of contaminants of emerging concern by UV-assisted homogeneous advanced oxidation/reduction processes. Sci. Total Environ. 899, 165625. https://doi.org/10.1016/J.SCITOTENV.2023.165625.

Villacorte, L.O., Boerlage, S., Dixon, M., 2021. Algal Blooms and RO Desalination. In: Salinas, S., Schippers, J., Amy, G., Kim, I., Kennedy, M. (Eds.), Seawater reverse osmosis desalination: assessment and pre-treatment of fouling and scaling. IWA Publishing. https://doi.org/10.2166/9781780409863.

Visciano, P., Schirone, M., Berti, M., Milandri, A., Tofalo, R., Suzzi, G., 2016. Marine biotoxins: occurrence, toxicity, regulatory limits and reference methods. Front. Microbiol. 7, 207058. https://doi.org/10.3389/FMICB.2016.01051/.

Wacławek, S., Grübel, K., Černík, M., 2015. Simple spectrophotometric determination of monopersulfate. Spectrochim. Acta - Part A Mol. Biomol. Spectrosc. 149, 928–933. https://doi.org/10.1016/j.saa.2015.05.029.

Yin, R., Ling, L., Shang, C., 2018. Wavelength-dependent chlorine photolysis and subsequent radical production using UV-LEDs as light sources. Water Res. 142, 452–458. https://doi.org/10.1016/J.WATRES.2018.06.018.

Zhou, C.Y., Pan, C.G., Peng, F.J., Zhu, R.G., Hu, J.J., Yu, K., 2024. Simultaneous determination of trace marine lipophilic and hydrophilic phycotoxins in various environmental and biota matrices. Mar. Pollut. Bull. 203, 116444. https://doi.org/10.1016/J.MARPOLBUL.2024.116444.

Zingone, A., Escalera, L., Aligizaki, K., Fernández-Tejedor, M., Ismael, A., Montresor, M., Mozetič, P., Taş, S., Totti, C., 2021. Toxic marine microalgae and noxious blooms in the Mediterranean Sea: a contribution to the Global HAB Status Report. Harmful Algae 102, 101843. https://doi.org/10.1016/J.HAL.2020.101843.